

Phase diagram of star-shaped polystyrene/cyclohexane system: location of critical point and profile of coexistence curve

H. Yokoyama, A. Takano, M. Okada* and T. Nose

Department of Polymer Chemistry, Tokyo Institute of Technology, Ookayama, Meguro-ku, Tokyo 152, Japan

(Received 20 August 1990; revised 28 September 1990; accepted 16 October 1990)

Coexistence curves of cyclohexane solutions of star-shaped polystyrenes (PSs) having 6.3 and 11.1 arms (arm molecular weight 1.88×10^5) were measured to investigate the effects of molecular shape on the phase diagram near the critical point. The reduced coexistence curve ϕ/ϕ_c versus τ/τ_c , where volume fraction ϕ and dimensionless temperature τ calculated from $\tau = (T - \Theta)/\Theta$ with a usual temperature T and the theta temperature Θ were reduced by the values at the critical point, were compared with those of linear PSs. The reduced coexistence curves of star-shaped PSs do not superpose on the reduced universal curve of linear PS when the same Θ is assumed for linear and star-shaped PSs. The critical temperature T_c and concentration ϕ_c were compared with those of linear, randomly branched, and comb-shaped PSs. The location of the critical point of the star-shaped PS is very different from that of linear PS of the same molecular weight M_w , indicating failure of the mean-field theory of polymer solutions. The same simple two-parameter scaling, which predicts the relations $\phi_c \sim \phi^*$ (= overlap concentration) and $\tau_c \sim (M_w \phi^*)^{-1}$, does not hold for the star-shaped and linear PSs, when the same Θ is used for linear and star-shaped PSs. The scaling relations do not hold either even when we use different Θ s for star-shaped PSs which were evaluated so that the reduced coexistence curves were superposed on the universal coexistence curve of linear PS. The ϕ_c of star-shaped PS lies at a lower concentration than expected from its ϕ^* and T_c lies at a lower temperature than expected from $(M_w \phi^*)^{-1}$.

(Keywords: star-shaped polystyrene; phase diagram; critical point; scaling theory)

INTRODUCTION

The investigation of the phase diagram of branched-polymer solutions is of fundamental importance in understanding the relation between microscopic segment correlation and macroscopic behaviour of polymer solutions, in addition to being of practical importance as a basis for the fractionation of a polymer mixture of various molecular shapes and weights. However, both theoretical and experimental studies on phase diagrams of branched-polymer solutions are still quite limited in number¹⁻³.

The mean-field theory of polymer solutions predicts that the critical polymer concentration expressed as a volume fraction ϕ_c and the critical temperature T_c depend on the degree of polymerization N :

$$\phi_c \sim N^{-1/2} \quad (1)$$

$$\tau_c \sim N^{-1/2} \quad (2)$$

for sufficiently large N . In equation (2), τ is the reduced temperature expressed with the theta temperature Θ by:

$$\tau = (T - \Theta)/\Theta \quad (3)$$

In scaling arguments neglecting higher order interactions than two, the free energy per site is written as:

$$F/kT = (a/R_g)^3 f(\phi/\phi^*, v/a^{-3} N^{-2} R_g^3) \quad (4)$$

where $f(x)$ is an unknown function, k is the Boltzmann constant, a is the statistical segment length, ϕ^* ($\sim a^3 N/R_g^3$) is the overlap concentration, R_g is the radius of gyration and v is the two-body interaction^{1,4}. The two-body interaction v is generally given as:

$$v \cong \tau \quad (5)$$

From equations (4) and (5), the following relations are derived for the critical point.

$$\phi_c \sim \phi^* \sim a^3 N/R_g^3 \quad (6)$$

$$\tau_c \sim (a^3 N^2/R_g^3)^{-1} \sim 1/N\phi^* \quad (7)$$

For linear polymers, equations (6) and (7) reduce to equations (1) and (2), respectively⁵, because $R_g \sim aN^{1/2}$ in the Θ region. Thus both the mean-field theory and the scaling theory give the same results regarding the molecular-weight dependence of ϕ_c and τ_c . However, it does not generally apply to branched polymers. Since polymers of different molecular shapes cannot be distinguished with the mean-field theory, the same critical point is predicted for both linear and branched polymers with the same molecular weights, as long as the very subtle contribution from the difference in chemical nature between monomer and branching unit is neglected. Consequently, the same molecular-weight dependence is given irrespective of molecular shapes. On the other hand, the scaling theory predicts the different critical points for linear and branched polymers depending on

* To whom correspondence should be addressed

their molecular dimensions R_g . For example, for randomly branched polymers, molecular-weight dependence is predicted to be different from equations (1) and (2), because the N dependence of R_g of randomly branched polymers is expressed¹ by a power different from 1/2. The mean-field approximation is known to be valid only in the concentrated region, but the critical point is located in the crossover region between dilute and semidilute⁵, so that it is not expected that the mean-field theory always predicts the correct location of the critical point.

In a previous paper², we studied the location of the critical point of a methylcyclohexane solution of randomly branched polystyrenes (PSs) by varying the molecular weight and the degree of branching. The location of the critical point and its molecular-weight dependence were found to be very different from those of linear polymers, showing a breakdown of the mean-field theory. In this study we investigate the effects of molecular shape on the location of the critical point using star-shaped polymers. Since a star-shaped polymer has a very different shape from a linear polymer and has a well-defined structure compared with a randomly branched polymer, it is a suitable sample for the investigation of the effects of molecular shape. When the degree of polymerization of an arm is fixed, R_g of a star-shaped polymer does not change so much with the number of arms f . Thus the molecular-weight dependence of the critical points of such star-shaped polymers forms a striking contrast with that of linear polymers according to equations (6) and (7).

We have measured coexistence curves of star-shaped PSs with arms of the same degree of polymerization in cyclohexane near their critical temperatures, and compared the obtained ϕ_c and T_c with data of linear, randomly branched and comb-shaped polymers. We also investigate the profile of the coexistence curve in the neighbourhood of the critical point. It is known that the profile of coexistence curves of linear polymers with various molecular weights can be scaled in a universal form in the neighbourhood of the critical point⁶⁻⁹. The critical amplitudes and profiles of coexistence curves of star-shaped polymers expressed with such scaled variables are examined by comparing with those for linear polymers.

EXPERIMENTAL

Samples

Star-shaped PSs were prepared by coupling living polystyryl anions on to a low molecular weight poly(4-vinylphenyldimethylvinylsilane) which had been previously anionically polymerized. Living polystyryl anions were end-capped with a few units of butadiene to reduce the influence of steric factors. An excess amount of the living arm polymers was added in the coupling reaction to ensure completion of the reaction. At each step of the sample preparation, a small amount of the sample was taken out of the reaction vessel to be subsequently characterized. After crude fractionation by the precipitation method using benzene and methanol, the star-shaped polymers were further fractionated with a preparative gel permeation chromatograph apparatus consisting of three columns (two G5000 H and one GMH; Tosoh Co.). The star-shaped PSs and their constituent arm and centre polymers were characterized by vapour pressure osmometry, membrane osmometry, sedimentation measurement, gel permeation chromatography and light scattering. Table 1 lists the characteristics of the star-shaped PS samples thus obtained. Non-integral numbers of arms indicate the existence of distribution in the number of arms, but the distribution is quite narrow since the sedimentation pattern showed a very sharp peak. Details of sample preparation and characterization will be described elsewhere¹⁰. Cyclohexane was dried over calcium hydride powder and purified by fractional distillation.

Concentrations of demixed phases were measured by a specially designed differential refractometer (Figure 1). A beam of light refracted from a solution in a Brice-type optical cell was detected at a particular channel on a photodiode array (image sensor). From the position of the channel detecting the refracted light, concentration was calculated by using calibration curves predetermined as functions of temperature. The incident laser beam was expanded in the vertical direction so that it could illuminate both the upper and lower phases of the demixed solution in the cell. Thus the concentrations of both phases were determined simultaneously without taking the solution out of the cell. In the case of the PS/cyclohexane solution, the concentration can be measured with this apparatus up to 25 wt% with an accuracy of ± 0.30 wt% in a temperature range from 20 to 60°C. The optical cell containing the sample solution and reference solvent was stoppered with Teflon plugs which were pressed tightly with a metal frame to prevent vaporization of the solvent and absorption of moisture for a couple of weeks. After a sample solution was homogenized above the critical temperature T_c , it was cooled down to a desired temperature below T_c and allowed to stand overnight to reach two-phase equilibrium. Temperature was controlled to within $\pm 0.02^\circ\text{C}$.

Coexistence curve measurement

Concentrations of demixed phases were measured by a specially designed differential refractometer (Figure 1). A beam of light refracted from a solution in a Brice-type optical cell was detected at a particular channel on a photodiode array (image sensor). From the position of the channel detecting the refracted light, concentration was calculated by using calibration curves predetermined as functions of temperature. The incident laser beam was expanded in the vertical direction so that it could illuminate both the upper and lower phases of the demixed solution in the cell. Thus the concentrations of both phases were determined simultaneously without taking the solution out of the cell. In the case of the PS/cyclohexane solution, the concentration can be measured with this apparatus up to 25 wt% with an accuracy of ± 0.30 wt% in a temperature range from 20 to 60°C. The optical cell containing the sample solution and reference solvent was stoppered with Teflon plugs which were pressed tightly with a metal frame to prevent vaporization of the solvent and absorption of moisture for a couple of weeks. After a sample solution was homogenized above the critical temperature T_c , it was cooled down to a desired temperature below T_c and allowed to stand overnight to reach two-phase equilibrium. Temperature was controlled to within $\pm 0.02^\circ\text{C}$.

Table 1 Characteristics of star-shaped PS samples

Sample	Molecular weight, M_w^a	Number of arms, f	Radius of gyration, R_g (nm) ^b
NF-1	1.20×10^6	6.3	22.5
NF-4	2.05×10^6	11.1	23.9

^a M_w of an arm: 1.88×10^5

^b In cyclohexane at 34.5°C

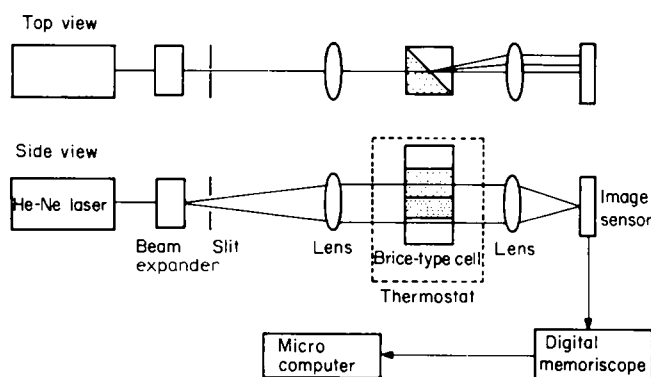


Figure 1 Schematic diagram of the differential refractometer for coexistence curve measurements

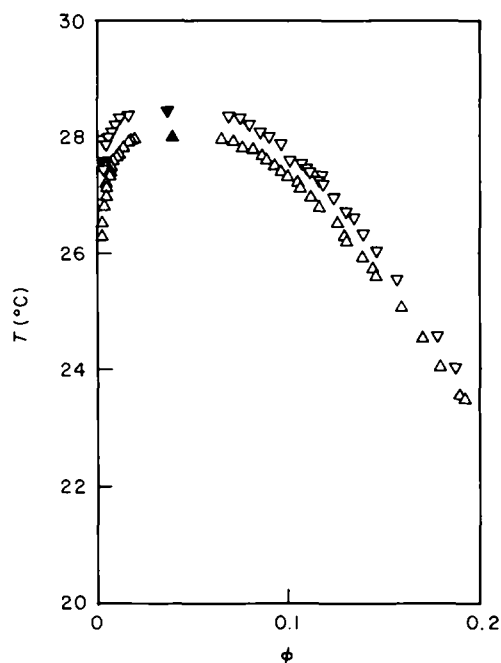


Figure 2 Coexistence curves for star-shaped PSs in cyclohexane: (Δ) NF-1; (∇) NF-4. Closed symbols indicate the critical points

RESULTS AND DISCUSSION

Coexistence curve and critical point

Figure 2 shows coexistence curves of star-shaped PSs in cyclohexane. The coexistence curve for each star-shaped polymer was determined with two different initial concentrations. Concentrations of coexistence phases which separated from different initial concentrations fall on a single curve within the experimental accuracy. This indicates that the effect of polydispersity can be neglected in the present system.

These data were fitted to the following universal form proposed by Chu and Wang⁸ for linear PS solutions:

$$\psi_c - \psi_d = A_d \varepsilon^\beta + B_d \varepsilon^{\beta + \Delta} \quad (8)$$

$$\psi_s - \psi_c = A_s \varepsilon^\beta + B_s \varepsilon^{\beta + \Delta} \quad (9)$$

$$\varepsilon \equiv |T - T_c|/T_c \quad (10)$$

where the dimensionless variable ψ , which is related to volume fraction ϕ through an adjustable parameter R as

$$\psi \equiv \frac{\phi}{\phi + R(1 - \phi)} \quad (11)$$

was introduced to symmetrize coexistence curves of polymer/solvent systems⁷. The subscripts c, d, and s of the variable ψ and the critical amplitudes A and B designate critical point, dilute phase and semidilute phase, respectively. The critical exponent β is fixed at the Ising value 0.327 and Δ is at 0.5. On the assumption of $A_d = A_s$, equations (8) and (9) yield

$$\psi_s + \psi_d = 2\psi_c + (B_s - B_d)\varepsilon^{\beta + \Delta} \quad (12)$$

$$\psi_s - \psi_d = 2A_d \varepsilon^\beta + (B_s + B_d)\varepsilon^{\beta + \Delta} \quad (13)$$

The data fitting was made in two steps. First, T_c was determined by plotting the concentration difference between two phases $\Delta\phi$ ($\equiv \phi_s - \phi_d$) to the power $1/\beta$ against T and extrapolating $(\Delta\phi)^{1/\beta}$ to zero. Then, the data of ϕ_s , ϕ_d and T were fitted to equations (10)–(13)

by the non-linear least squares method with A_d , B_d , B_s , and R taken as parameters. We arbitrarily set $\psi_c = 0.25$, the same as in case of linear PSs⁸. The T_c and the parameters thus obtained are listed in Table 2.

For linear PSs in cyclohexane, Chu and Wang⁸ have evaluated these parameters as functions of N ($= M_w/104$) using the data by Nakata *et al.*^{11,12}:

$$A_d(\ln) = 0.595N^{0.1014} \quad B_d(\ln) = -0.425N^{0.2564}$$

$$B_s(\ln) = 0.018N^{0.2564}$$

These relations give for the same molecular weight as NF-1:

$$A_d(\ln) = 1.564 \quad B_d(\ln) = -4.89 \quad B_s(\ln) = 0.21$$

and for the same molecular weight as NF-4:

$$A_d(\ln) = 1.651 \quad B_d(\ln) = -5.62 \quad B_s(\ln) = 0.24$$

The amplitude A_d for the star-shaped polymers is slightly larger than that of the linear polymers (Table 2). The critical amplitude A , which is defined with volume fraction as $\Delta\phi = A\varepsilon^\beta$, can be calculated from A_d as follows. Substitution of equations (8), (9) and (11) into the definition of A

$$A = \lim_{\varepsilon \rightarrow 0} \frac{\Delta\phi}{\varepsilon^\beta} \quad (14)$$

yields

$$A = \frac{2A_d\phi_c(1 - \phi_c)}{\psi_c(1 - \psi_c)} \cong 10.67A_d\phi_c(1 - \phi_c) \quad (15)$$

For star-shaped PSs, we obtain $A = 0.740$ for NF-1 and $A = 0.751$ for NF-4 by using the values of Table 2. The critical concentrations ϕ_c of linear PSs in cyclohexane have been formulated as a function of molecular weight in reference 8. By using ϕ_c calculated from the formula and A_s s shown above, we obtain $A = 0.528$ and 0.457 for the linear PSs of the same molecular weights as NF-1 and NF-4, respectively. The critical amplitude A of the star-shaped PS is about 1.5 times larger than that of the linear PS of the same M_w . The difference in A between linear and star-shaped PSs is larger than the difference in A_d , because the difference in molecular shape is reflected in A through ϕ_c .

Coexistence curves of linear PS solutions of various molecular weights are known⁶ to be scaled onto a universal curve when they are plotted with reduced variables ϕ/ϕ_c and τ/τ_c . We attempt to test whether the universality exists among the polymers of different molecular shapes. To calculate the reduced temperature τ from T , we need to evaluate the Θ temperature of star-shaped PS. Here we use the same value for the Θ temperature of star-shaped PS as that for linear PS ($\Theta = 34.5^\circ\text{C}$) because the two-body interaction is generally considered to be independent of molecular shape and

Table 2 Characteristic parameters of the coexistence curve for star-shaped PSs

Sample	T_c (°C)	ϕ_c (vol. fraction)	R	A_d	B_d	B_s
NF-1	28.0	0.0393	0.1226	1.836	-8.20	-3.26
NF-4	28.4	0.0371	0.1155	1.970	-7.95	-3.62

$A_s = A_d$; $\psi_c = 0.25$

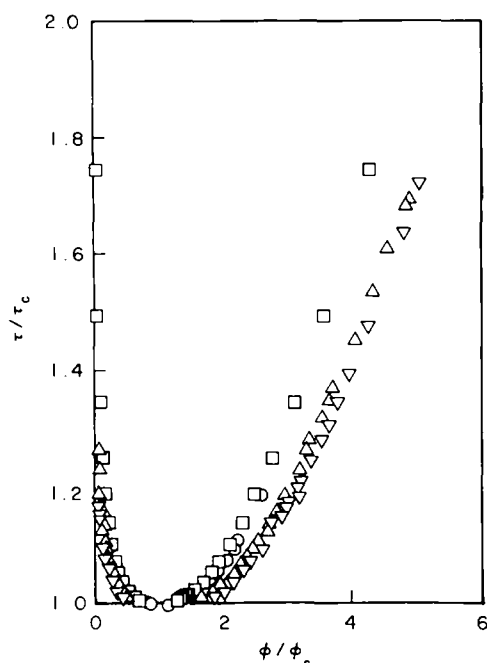


Figure 3 Reduced coexistence curves of star-shaped and linear PSs in cyclohexane: (Δ) NF-1; (∇) NF-4; (\circ) linear¹¹, $M_w = 2.0 \times 10^5$; (\square) linear¹², $M_w = 1.56 \times 10^6$

weight, which implies that the Θ temperature of star-shaped PS should be equal to that of linear PS within the framework of the treatment shown above (see equation (5)). Coexistence curves of star-shaped and linear^{11,12} PSs are plotted with the reduced quantities ϕ/ϕ_c and τ/τ_c in Figure 3. The reduced coexistence curves of the star-shaped polymers obviously deviate from the universal curve of the linear polymers. It appears that the amplitude of $\Delta\phi/\phi_c$ increases with increasing number of arms: the curves of the star-shaped polymers are located outside the universal curve of the linear polymers, and the curve of the star-shaped polymer with the larger number of arms is slightly broader than that with the smaller number of arms. These results show that the coexistence curves of homologous polymers of different molecular shapes do not scale in a single universal form as long as the same Θ temperature is assumed for these polymers. It is not clear whether the observed deviation arises from lack of the universality of coexistence curves among the polymers of different shapes or from the molecular-shape dependence of the Θ temperature. We measured the second virial coefficients A_2 of cyclohexane solutions of star-shaped PSs at several temperatures near 34.5°C by using the light scattering technique, but could not evaluate the Θ temperature with sufficient accuracy because A_2 has a very small temperature dependence in this region. Conflicting experimental results have been reported for the Θ temperature of star-shaped polymers. The Θ temperature determined as the temperature at which A_2 vanishes, is known to be lower than that of the linear polymer in the same solvent when the M_w of the arm is not large¹³, but is identical if the M_w of the arm is sufficiently large ($M_w \geq 10^5$ when the number of arms is not very large)^{14,15}. On the other hand, the Θ temperature determined as the critical solution temperature of a polymer of infinitely large molecular weight is slightly lower than the Θ temperature of a linear homologue³.

Molecular-weight dependence of ϕ_c and τ_c

Figures 4 and 5 show the molecular-weight dependence of ϕ_c and τ_c for star-shaped and linear PSs in cyclohexane. For comparison, the data of methylcyclohexane solution of linear, randomly branched and comb-shaped PSs are also shown. The values of ϕ_c and τ_c for linear PSs were calculated from the empirical equations obtained by Perzynski *et al.*¹⁶ and Chu and Wang⁸. The results of

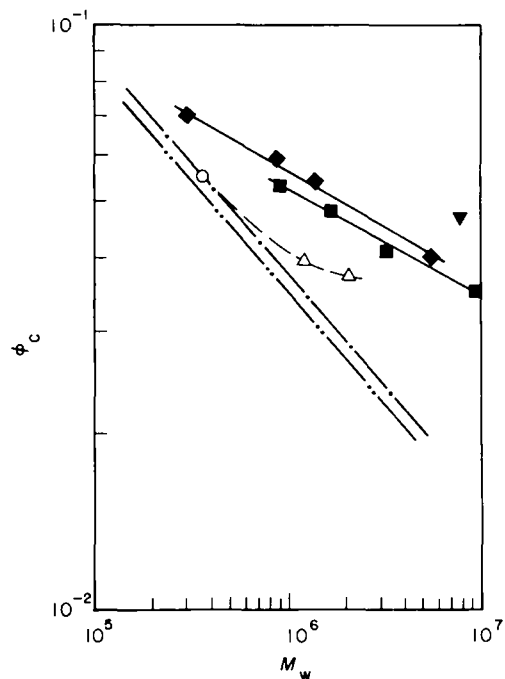


Figure 4 Molecular-weight dependence of critical concentration ϕ_c of PSs: in cyclohexane, (Δ) star-shaped; (—) linear^{8,16}; in methylcyclohexane, (---) linear⁸; (\blacksquare) randomly branched² with degree of branching DVB/St = 1/1000 molar ratio; (\blacklozenge) randomly branched² with St/DVB = 500/1; (\blacktriangledown) comb-shaped. Circle (\circ) corresponds to star-shaped PS with two arms

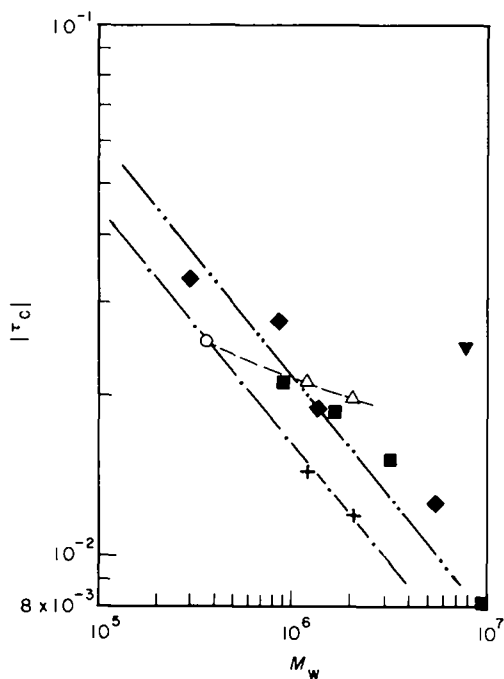


Figure 5 Molecular-weight dependence of $|\tau_c|$ for various-shaped PSs: (—) star-shaped PS calculated with $\Theta = 32.4$ and 32.1°C. The other symbols are the same as in Figure 4

randomly branched PSs have been reported previously². These randomly branched PSs were prepared by copolymerization of styrene (St) and a branching agent *p*-divinylbenzene (DVB) in molar ratios of 500:1 and 1000:1. The anionically polymerized comb-shaped PS consists of a stem of $M_w = 3.68 \times 10^5$ and 118 branches of a uniform length ($M_w = 6.32 \times 10^4$). Again, we assumed that the Θ temperatures of these branched polymers are the same as that of the homologous linear polymers in calculating the reduced temperature τ .

The Flory-Huggins theory gives the same critical point to polymers of the same molecular weight in the same solvent regardless of their molecular shapes. However, regarding the critical concentration ϕ_c , none of the data points of branched PSs fall on the lines of linear PSs. The critical concentration is obviously increased by branching. The critical temperature τ_c of randomly branched PS does not change so much with the degree of branching in contrast with the critical concentration ϕ_c , and deviation from the linear polymers is not clearly observed due to relatively large experimental scatter. In contrast with this, τ_c of star-shaped PS largely deviates from the τ_c - M_w relation of linear PS. The critical temperature T_c of star-shaped PS is lower than T_c of linear PS of the same molecular weight, which is consistent with the results by Cowie *et al.*³ for the upper critical solution temperatures of PS-cyclohexane systems. The validity of the assumption that the Θ temperature of branched PS is identical to that of linear PS is not clear as mentioned above. If the Θ temperatures of star-shaped PSs are determined so that the reduced coexistence curves of both polymers fall on the universal curve of linear PS at an arbitrarily chosen concentration $\phi/\phi_c = 4$, we obtain $\Theta = 32.4^\circ\text{C}$ for NF-1 and $\Theta = 32.1^\circ\text{C}$ for NF-4. When these values are used, the reduced critical temperatures τ_c of the star-shaped PSs fall on the line of linear PS.

Relationship of ϕ_c and τ_c to chain dimension R_g

In the recent theories of polymer solutions, which take into account the correlation of segment density caused by connectivity of segments, chain dimension plays an important role in describing solution properties, as seen in equation (4) for example. Figure 6 shows the R_g of various shaped PSs at the Θ temperatures of linear PS as functions of M_w . The R_g of randomly branched PSs can be also expressed by the power law $R_g \sim N^\nu$, and the exponent $\nu = 0.38$ – 0.40 is smaller than that of the linear polymers ($\nu = 0.5$). The R_g of the star-shaped PS with a fixed arm length changes only slightly with the number of arms. From Figure 6, it appears that the R_g decrease in an order linear > randomly branched > comb-shaped > star-shaped PSs when they are compared at a fixed molecular weight. Consequently, segment densities $a^3 N R_g^{-3}$ ($\sim \phi^*$) inside polymer coils increase in the reverse order at a fixed molecular weight.

To see applicability of the scaling relation expressed by equation (6), the critical concentrations ϕ_c are plotted against ϕ^* in a double logarithmic scale in Figure 7. Data points of the randomly branched polymers fall approximately on the straight line of the linear polymer, whereas those of the comb-shaped and star-shaped polymers deviate seriously from the line. The critical concentration of the star-shaped polymers is located at a lower concentration than that expected from the overlap concentration ϕ^* , and the polymer with the larger

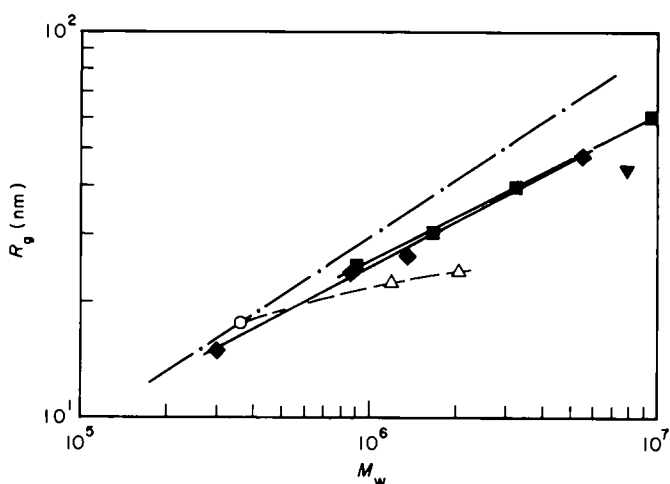


Figure 6 Molecular-weight dependence of radius of gyration R_g for various-shaped PSs at the Θ temperatures of linear PS: (---) linear; (Δ) star-shaped; (\circ) star-shaped (two arms); (\blacksquare) randomly branched (DVB/St=1/1000); (\blacklozenge) randomly branched (St/DVB=500); (\blacktriangledown) comb-shaped

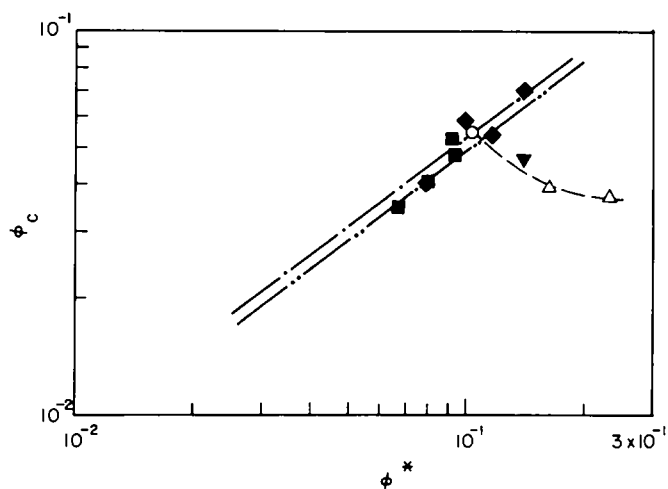


Figure 7 Double logarithmic plots of ϕ_c versus ϕ^* for various-shaped PSs. The symbols are the same as in Figure 4

number of arms shows the larger deviation. The deviation of comb-shaped PS from the line of linear PS is smaller than the deviation of star-shaped PS, which is in contrast to the plot of ϕ_c versus M_w (Figure 5), where comb-shaped PS shows the largest deviation from the line of linear PS. The deviation increases in the order of increasing segment density inside a polymer coil. It seems that ϕ_c is not simply determined by the average segment density ϕ^* inside a polymer coil, but that it also depends on the segment distribution inside the coil. It should be noted that the slope of the linear PS data in the double-logarithmic scale apparently deviates from unity. Figure 7 indicates that equation (6) should be replaced by:

$$\phi_c \sim (\phi^*)^\alpha \quad \alpha \cong 0.76 \quad (6a)$$

The reduced critical temperature τ_c is plotted against $(M_w/\rho N_A)^2/R_g^3 \propto N^2 R_g^{-3}$, where ρ is density of PS and N_A is the Avogadro constant, in Figure 8 to examine applicability of equation (7). The line of the linear PS data has a slope nearly equal to unity, which agrees with equation (7). However, no data of the branched polymers fall on the lines of the linear polymers, including the

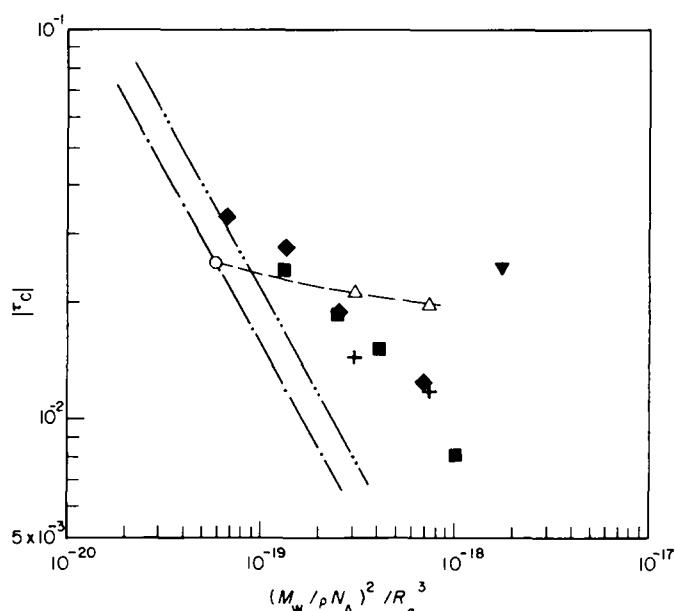


Figure 8 Double logarithmic plots of $|c_c|$ versus $(M_w / \rho N_A)^2 / R_g^3$ for various-shaped PSs. The symbols are the same as in Figure 5.

randomly branched polymers whose critical concentrations have been approximately scaled on to the line of the linear polymer. The critical temperature τ_c appears to be more sensitive to the molecular shape than the critical concentration ϕ_c . Even when the Θ temperature determined so as to give the universal coexistence curve in Figure 3 is used in the calculation of τ_c , the reduced critical temperatures τ_c of star-shaped PSs do not fall on the line either.

Contribution of three-body interaction

Since equations (6) and (7) were proposed for randomly branched polymers and there is no reason to assume that they are applicable to star-shaped polymers, it is not surprising that the results of the star-shaped polymers deviate from these equations. The experimental study on the osmotic pressure π by Higo *et al.*¹⁷ has also shown that branched polymers do not follow the same scaling relation as that of linear polymers: the osmotic pressures π of linear polymers of various molecular weights are known to be scaled by the relation $\pi N / \phi k T = f(\phi / \phi^*)$, but the data of comb-shaped polymers deviate from the relation of linear polymers. In addition, even linear polymers do not follow equation (6) exactly. These facts suggest that equation (4) is inappropriate for the universal scaling form applicable to polymers of different molecular shapes. A simplification made in equation (4) is to neglect higher order interactions. However, the higher-order interaction cannot be neglected in the Θ region where two-body interaction becomes very small. To estimate the contribution from the higher-order interaction, we calculate the critical point based on a simple classical expression, in a reduced form, of free energy containing up to three-body interaction ω as:

$$\begin{aligned} \frac{F}{kT} &= \frac{\phi}{N} \ln \left(\frac{\phi}{\phi^*} \right) + v\phi^2 + \omega\phi^3 \\ &= \left(\frac{a}{R_g} \right)^3 \left[\frac{\phi}{\phi^*} \ln \left(\frac{\phi}{\phi^*} \right) + \frac{va^3 N^2}{R_g^3} \left(\frac{\phi}{\phi^*} \right)^2 + \frac{\omega a^6 N^3}{R_g^6} \left(\frac{\phi}{\phi^*} \right)^3 \right] \\ &= \left(\frac{a}{R_g} \right)^3 (\tilde{\phi} \ln \tilde{\phi} + \tilde{v}\tilde{\phi}^2 + \tilde{\omega}\tilde{\phi}^3) \end{aligned} \quad (16)$$

where the reduced quantities were defined as $\tilde{\phi} = \phi / \phi^*$, $\tilde{v} = v / (a^{-3} N^{-2} R_g^3)$, and $\tilde{\omega} = \omega / (a^{-6} N^{-3} R_g^6)$. The three-body interaction parameter ω is generally assumed to be independent of T and N . This equation yields:

$$\tilde{\phi}_c = (6\tilde{\omega})^{-1/2} \quad (17)$$

$$\tilde{v}_c = -(6\tilde{\omega})^{1/2} \quad (18)$$

which reduce to

$$\phi_c = (6\omega N)^{-1/2} \quad (17a)$$

$$\tau_c = -(6\omega / N)^{1/2} \quad (18a)$$

These equations are independent of R_g and thus cannot explain the observed molecular-shape dependence. The coexistence curve in the vicinity of the critical point is calculated from equation (16) by the relation¹⁸:

$$(\Delta\phi)^2 = 6 [(\partial^3 F / \partial T \partial \phi^2)_c] / (\partial^4 F / \partial \phi^4)_c]$$

to be

$$\Delta\phi / \phi_c = (-6\tilde{\phi}_c \tilde{v}_c)^{1/2} (\tau / \tau_c)^{1/2} = \sqrt{6} (\tau / \tau_c)^{1/2} \quad (19)$$

The exponent 1/2 is obtained as a consequence of the classical expression used in equation (16). More important is that the critical amplitude \tilde{A} of the scaled coexistence curve $\Delta\phi / \phi_c$ versus τ / τ_c is independent of ω . Therefore no improvement is made by introducing a new scaling equation (16). Equations (17a), (18a) and (19) show that the three-body interaction parameter cannot explain the breakdown of the simple scaling form of equation (4) for either the location of the critical point or the profile of the coexistence curve.

When we take into account the higher order interactions, we have to distinguish two Θ temperatures, i.e. the renormalized Θ temperature at which the apparent two-body interaction disappears and the bare Θ temperature at which the real two-body interaction disappears^{5,13}. We have developed our discussion mainly based on the bare Θ temperature. The chemical potential μ may be written as¹⁹:

$$\mu / 2\phi k T = v + (3/2)\omega\phi \equiv v' = \tau' = (T - \Theta') / \Theta' \quad (20)$$

from which we can calculate renormalized two-body interaction v' and renormalized Θ temperature Θ' . For the concentration ϕ in equation (20), we should use the radial distribution function $g(r)$ at $r \cong a$ instead of the average concentration inside a polymer coil $a^3 N / R_g^3$ according to de Gennes¹⁹. Since $g(r \cong a)$ is considered to be larger in star-shaped polymers than in linear polymers, the renormalized Θ temperature would be reduced. This is consistent with the fact that the Θ temperature determined so as to give a universal phase diagram is lower than the Θ temperature of linear PS. This suggests that deviation from the universality among various-shaped polymers may be improved by using an experimentally determined renormalized Θ temperature. However, the Θ temperature which satisfies the universal coexistence curve could not satisfy the scaling relation equation (7) as seen in Figure 8. Thus, it does not appear that the universal relation will hold among various-shaped polymers by using the renormalized Θ temperature.

ACKNOWLEDGEMENT

We wish to thank Dr Fujimoto of Nagaoka Technical

University for providing the anionically polymerized comb-shaped PS.

REFERENCES

- 1 Daoud, M., Pincus, P., Stockmayer, W. H. and Witten, T. *Macromolecules* 1983, **16**, 1833
- 2 Satoh, S., Okada, M. and Nose, T. *Polym. Bull.* 1985, **13**, 277
- 3 Cowie, J. M. G., Horta, A., McEwen, I. J. and Prochazka, K. *Polym. Bull.* 1979, **1**, 329
- 4 Daoud, M. and Jannink, G. *J. Phys. (Les Ulis, Fr.)* 1976, **37**, 973
- 5 de Gennes, P. G. 'Scaling Concepts in Polymer Physics', Cornell University Press, Ithaca, 1979
- 6 Izumi, Y. and Miyake, Y. *J. Chem. Phys.* 1984, **81**, 1501
- 7 Sanchez, I. C. *J. Appl. Phys.* 1985, **58**, 2871
- 8 Chu, B. and Wang, Z. *Macromolecules* 1988, **21**, 2283
- 9 Mel'nichenko, Yu. B. and Klepko, V. V. *J. Phys. (Les Ulis, Fr.)* 1989, **50**, 1573
- 10 Takano, A., Okada, M. and Nose, T. *Polymer* in press
- 11 Nakata, M., Kuwahara, N. and Kaneko, M. *J. Chem. Phys.* 1975, **62**, 4278
- 12 Nakata, M., Dobashi, T., Kuwahara, N., Kaneko, M. and Chu, B. *Phys. Rev. A* 1978, **18**, 2683
- 13 Candau, F., Rempp, P. and Benoit, H. *Macromolecules* 1972, **5**, 627
- 14 Roovers, J. E. L. and Bywater, S. *Macromolecules* 1974, **7**, 433
- 15 Bauer, B. J., Hadjichristidis, N., Fetters, L. J. and Roovers, J. E. L. *J. Am. Chem. Soc.* 1980, **102**, 2410
- 16 Perzynski, R., Delsanti, M. and Adam, M. *J. Phys. (Les Ulis, Fr.)* 1987, **48**, 115
- 17 Higo, Y., Ueno, N. and Noda, I. *Polym. J.* 1983, **15**, 367
- 18 Landau, L. D. and Lifshitz, E. M. 'Statistical Physics Part 1', 3rd Edn, Pergamon Press, Oxford, 1980, Ch. XIV
- 19 de Gennes, P. G. 'Scaling Concepts in Polymer Physics', Cornell University Press, Ithaca, 1979, p. 116